Scanning Microscopy

Volume 8 | Number 4 Article 4

12-22-1994

Metastable Reconstructions on Si(111)

Y. -N. Yang
University of Maryland

E. D. Williams
University of Maryland

Scanning Microscopy, Vol. 8, No. 4, 1994 (Pages 781-794) 0891-7035/94$5.00+.25
Scanning Microscopy International, Chicago (AMF O'Hare), IL 60666 USA

METASTABLE RECONSTRUCTIONS ON Si(111)

Y.-N. Yang and E.D. Williams*

Department of Physics and Institute for Physical Science and Technology
University of Maryland, College Park, MD 20742-4111

(Received for publication May 10, 1994 and in revised form December 22, 1994)

Abstract

We report unambiguous atomic scale evidence demonstrating that the atom density in the high temperature "1x1" phase of Si(111) is ~6% higher than the 7x7. Such evidence is provided by scanning tunneling microscopy (STM) observation of excess adatom density, and related island formation, on surfaces with very large terraces. The unusually large terraces were produced by heating the sample with DC current in the step-down direction at 1200°C. By trapping adatoms on the terraces through a quench, we have also created areas of metastable reconstructions, i.e., 9x9, 2x2, c2x4 and $\sqrt{3}$x$\sqrt{3}$, much larger than previously reported. For the first time, we have demonstrated the existence of metastable 11x11, 13x13 and c2x8 on Si(111). We have found that the c2x8 reconstruction can be stabilized as well as other members of the 2x2/c2x4/c2x8 family of reconstructions. An energetic model, based on the idea of atomic conservation, is proposed for the formation of the observed high atom density metastable reconstructions.

Key Words: Si(111), silicon, surface reconstruction, scanning tunneling microscopy (STM), surface energy, homo-epitaxy, electromigration.

*Address for correspondence:
Ellen D. Williams
Department of Physics,
University of Maryland,
College Park, MD 20742-4111
Telephone number: (301) 405-6156
FAX number: (301) 314-9465

Introduction

As one of the most studied semiconductor surfaces, it has been firmly established, both experimentally (Schlier and Farnsworth, 1959; Lander, 1964; Bennett and Webb, 1981; Becker *et al.*, 1985; Hamers *et al.*, 1986) and theoretically (Vanderbilt, 1987; Brommer *et al.*, 1992; Stich *et al.*, 1992), that Si(111) has a 7x7 reconstruction of Takayanagi type (Takayanagi *et al.*, 1985) after thermal annealing at high temperature (> 600°C). In addition to this energetically favored structure, other metastable structures have also been reported. It is well known that cleaved Si(111) exhibits a 2x1 reconstruction given by the p-bonded chain model (Pandey, 1981). Using scanning tunneling microscopy (STM), Becker *et al.* (1986) reported a host of new reconstructions, i.e., 9x9, 5x5, 2x2, c2x4 and $\sqrt{3}$x$\sqrt{3}$, on laser-annealed clean Si(111). However, it was not clear what caused these structures to form. A common feature of most of the new reconstructions observed in Becker's experiment was a higher atom density than that of the 7x7. As we will show in the following, the formation of these structures is likely to be a result of the surface trying to accommodate the high density of adatoms formed by laser annealing.

As we have recently demonstrated (Yang and Williams, 1994), one tool available to help probe the metastable structures on Si(111) is the high temperature phase. Compared to the large amount of work that has been done on the low temperature structures (< 830°C) of Si(111), particularly the 7x7, little is known about the "1x1" phase of Si(111) at high temperature. The notation "1x1" comes from the early observations of 1x1 symmetry in the diffraction pattern for the phase. More recently, both diffuse 2x2 and $\sqrt{3}$x$\sqrt{3}$ low energy electron diffraction (LEED) patterns have been reported for the phase (Ino, 1977; Iwasaki *et al.*, 1987; Phaneuf and Williams, 1987). The two new observed LEED patterns seem to suggest the existence of a weakly ordered overlayer and thus a higher atom density than that of the bulk terminated surface. It has also been reported on the basis of reflection electron microscopy (REM) measurements that the structural transition of "1x1" to

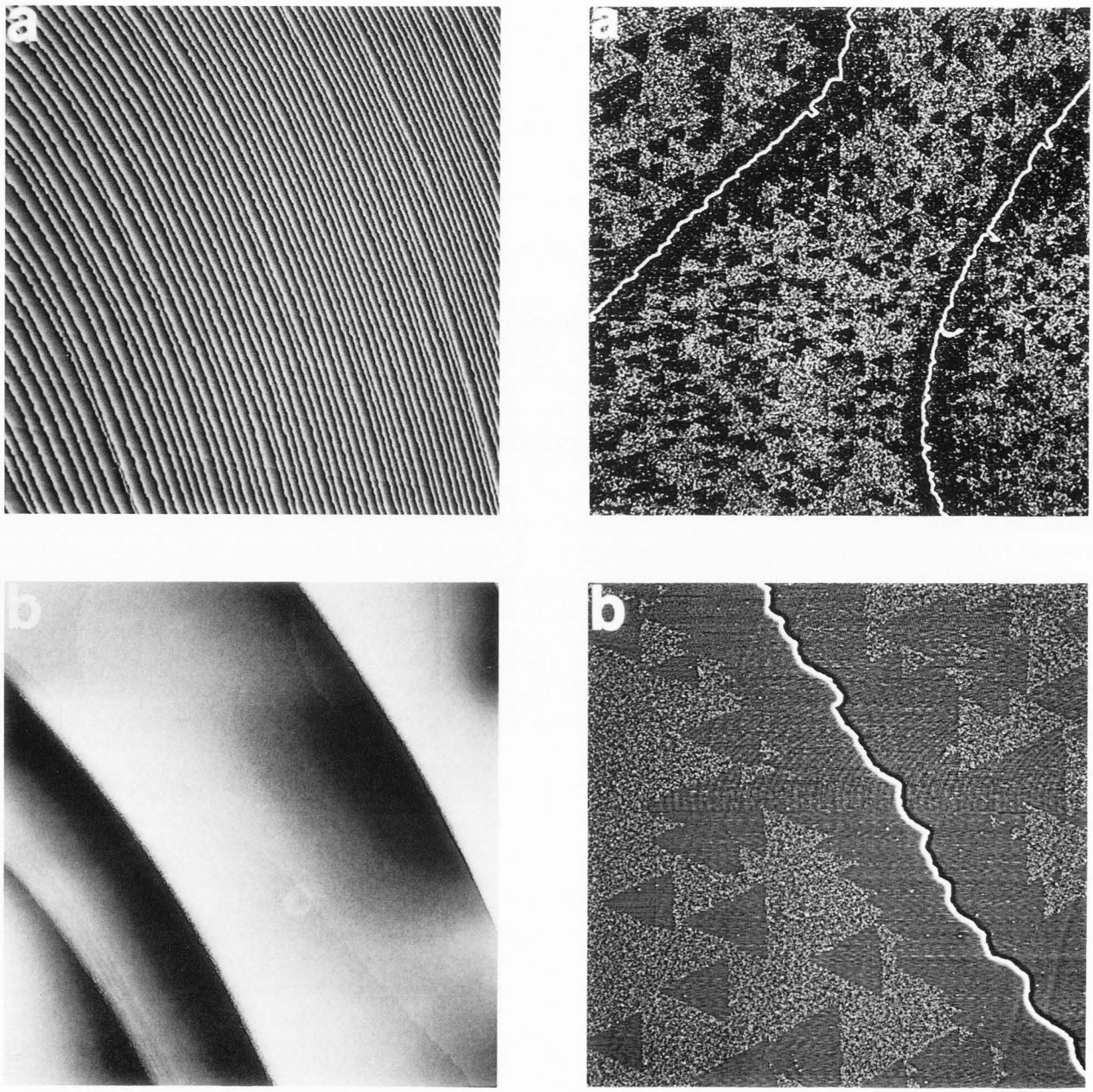

Figure 1. STM images of area 6000 nm x 6000 nm after annealing at 1200°C for 3 minutes using (**a**) DC current in step-up direction and (**b**) DC current in the step-down direction. Large terraces are created by annealing using step-down current. The curved appearance of the steps is due to distortions in the piezo electric tube scanner.

7x7 results in a net displacement of the step edges (Latyshev *et al.*, 1991). The implication of these data is that the high temperature phase has higher density than the 7x7 and that the excess atoms, released when the lower density 7x7 forms, diffuse to the step edge.

In this paper, we report clear experimental evidence showing that the atom density of the "1x1" phase is indeed higher than that of the 7x7. We demonstrate this by imaging, with STM, Si(111) surfaces quenched from the "1x1" into the 7x7 on unusually large terraces created using electromigration. Furthermore, we demonstrate that we can use high atom density in the "1x1" phase to create larger areas of 9x9, 2x2/c2x4/c2x8 and $\sqrt{3}x\sqrt{3}$ than have been previously reported, by controlling the cooling rate relative to the terrace size. Also on such surfaces, for the first time, we have observed 11x11, c2x8 and possibly 13x13 reconstructions. We propose a simple energetic argument, as opposed to kinetic, to

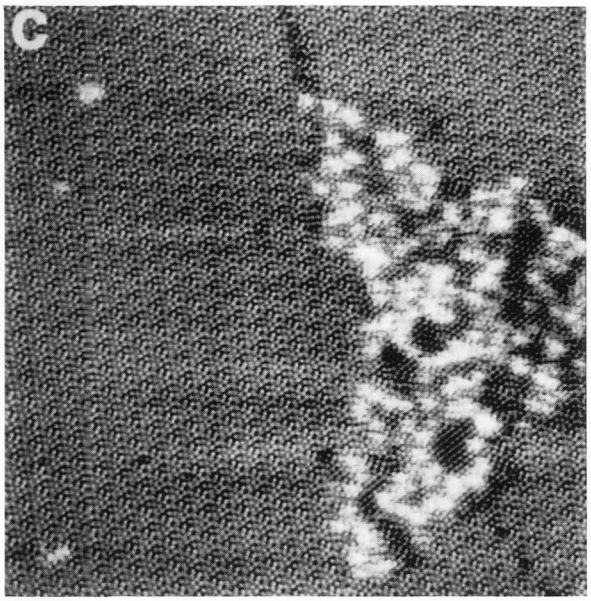

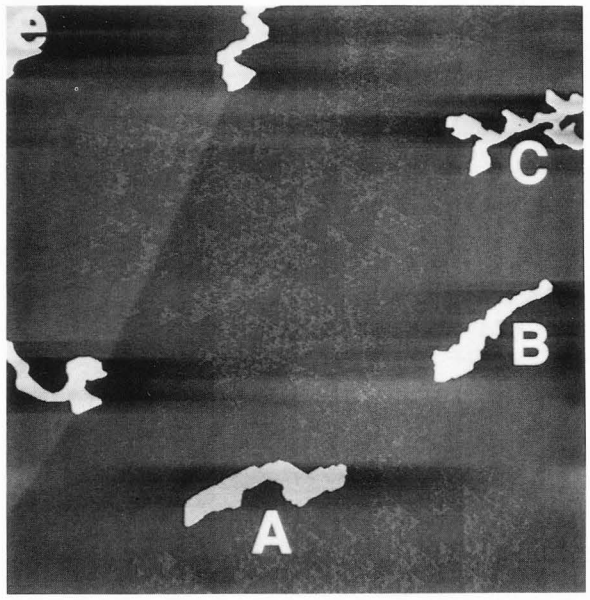

Figure 2 (a and b are on the facing page, column 2). **(a)** 4500 nm x 4500 nm STM scan of Si(111) after quench from 900°C showing dark 7x7 triangular domains and regions with clouds of adatoms that have a brighter gray scale. Depletion zones near step edges are also evident. Steps in the image are single height steps. Terrace on the left of a step is higher than that on the right. **(b)** 1500 nm x 1500 nm close-up view of a region near a step. Images in (a) and (b) have been filtered to emphasize adatoms trapped on the large terrace created using electromigration. **(c)** 75 nm x 75 nm image showing 7x7 domains and atomic structures in the cloudy region. **(d)** 6000 nm x 6000 nm image of a surface after annealing at 600°C following quench. The formation of islands on the surface provides clear evidence that the atom density of "1x1" is higher than that of the 7x7. **(e)** Close image (2000 nm x 2000 nm) of the reannealed surface showing remaining "cloudy" region and depletion zone around each island. The sample bias for all images was +2 V.

---

show that the formation of these non-7x7 reconstructions are a result of the presence of a higher than equilibrium atom density on the surface during the quench.

Experimental

The experiments were performed in an ultra high vacuum (UHV) system with a base pressure of 2 x 10^{-11} Torr equipped with a homemade scanning tunneling microscope. Nominally flat Si(111), n-type, phosphorus doped wafers, 15 mm x 3 mm x 0.4 mm in size, were installed in vacuum without chemical precleaning. After being degassed at 700°C, the cleanliness of the surfaces was ensured by flashing to 1250°C for 1 minute. The samples were then annealed for a chosen time at 1200°C as discussed below, then quickly cooled to 900°C and quenched from this temperature to below 250°C with a cooling rate of ~100°C/s by cutting off the heating current. The temperature of the sample was measured using an infrared (IR) pyrometer.

The fast cooling rate used to quench the surfaces was achieved by reducing the thermal mass of the heater using direct current (DC) heating. The second benefit of DC heating is that the "electromigration" effect can be used to control the step structure on the surface (Latyshev *et al.*, 1989; Homma *et al.*, 1990; Alfonso *et al.*, 1992; Noh *et al.*, 1993; Yang and Williams, 1994).

Table 1. The density of Si atoms per 1x1 area of the surface double layer for different reconstructions.

Surface Reconstruction	Density (atoms/ unit cell)	% difference relative to 1x1	References
1x1	2	0	-
2x1	2	0	Feenstra and Lutz, 1991b; this work.
5x5	2	0	Becker, *et al.*, 1986; Feenstra and Lutz, 1991b; Hoegen *et al.*, 1989; Kohler *et al.* 1989; this work.
7x7	2.08	4.1	Becker *et al.*, 1985; Hamers *et al.*, 1986; this work.
9x9	2.12	6.2	Becker *et al.*, 1986; Feenstra and Lutz, 1991a; this work
11x11	2.15	7.4	this work
13x13	2.17	8.3	this work
"1x1"	2.20-2.22 (measured)	10-11(measured)	this work
2x2, c2x4	2.25	12.5	Becker *et al.*, 1986; this work.
$\sqrt{3}x\sqrt{3}$	2.33	16.7	Becker *et al.*, 1986; this work.

Figure 1a shows a Si(111) surface with a uniform step train after annealing the sample at 1200°C for 3 minutes using DC current in the step-up direction. Figure 1b shows the same sample after annealing at 1200°C for 3 minutes when the DC current is in the step-down direction. Big step bunches, each having more than 20 single steps, are shown in Figure 1b. These bunches are separated by terraces as large as 3000 nm wide. Several trapped single height steps are found on the large terraces. For this work, we annealed the sample until the distances between step bunches were larger than the 6000 nm field of view of our STM. Consequently, the separation between trapped single height steps was ~2000 nm. The accumulative annealing time needed to achieve the required terrace size is about 8 minutes.

Results and Discussion

The "1x1" phase has higher atom density than 7x7

When the temperature of a Si(111) surface is slowly lowered from the "1x1" phase into the 7x7 phase, the 7x7 nucleates at the top of step edges and grows across the terraces (Bauer *et al.*, 1991). In such a case, the excess atoms in the "1x1" phase, as suggested by the REM measurements, should diffuse to the step edges and become indistinguishable from the rest of the surface. On the other hand, a rapid quench from high temperature might be able to trap the adatoms on the terrace. For this to succeed, the time it takes to quench to low temperature must be shorter than the time it takes for the adatoms to diffuse across the terraces to the steps. However, the ultra-fast cooling rates achieved using laser annealing are not desirable, as such fast cooling prohibits the formation of the 7x7 (Becker *et al.*, 1986). The best way to trap the adatoms on the terraces, yet still allow the 7x7 to form, is to quench surfaces with **large terrace widths**, at a moderate speed.

Figure 2a shows a 4500 nm x 4500 nm scan of a surface quenched from 900°C with a rate of ~100°C/s. The image has been filtered to emphasize features on the terraces. As a result, the two single-height steps in the field of view appear as two bright lines in the image. It is evident that in addition to the dark triangular regions, which close-up images show to contain a well-ordered 7x7, there are regions which appear to have overlying "clouds" on the surface. We will show these regions contain trapped Si adatoms. A close-up of a region near a step edge is shown in Figure 2b. It is clear from Figures 2a and 2b that there is a depletion zone of the cloudy structure on both sides of the step edge. Atomically resolved images (as in the triangular region shown in Fig. 2c) show that the reconstruction within this zone is entirely 7x7. This suggests that any adatoms initially found near the step edges diffused to the step and were

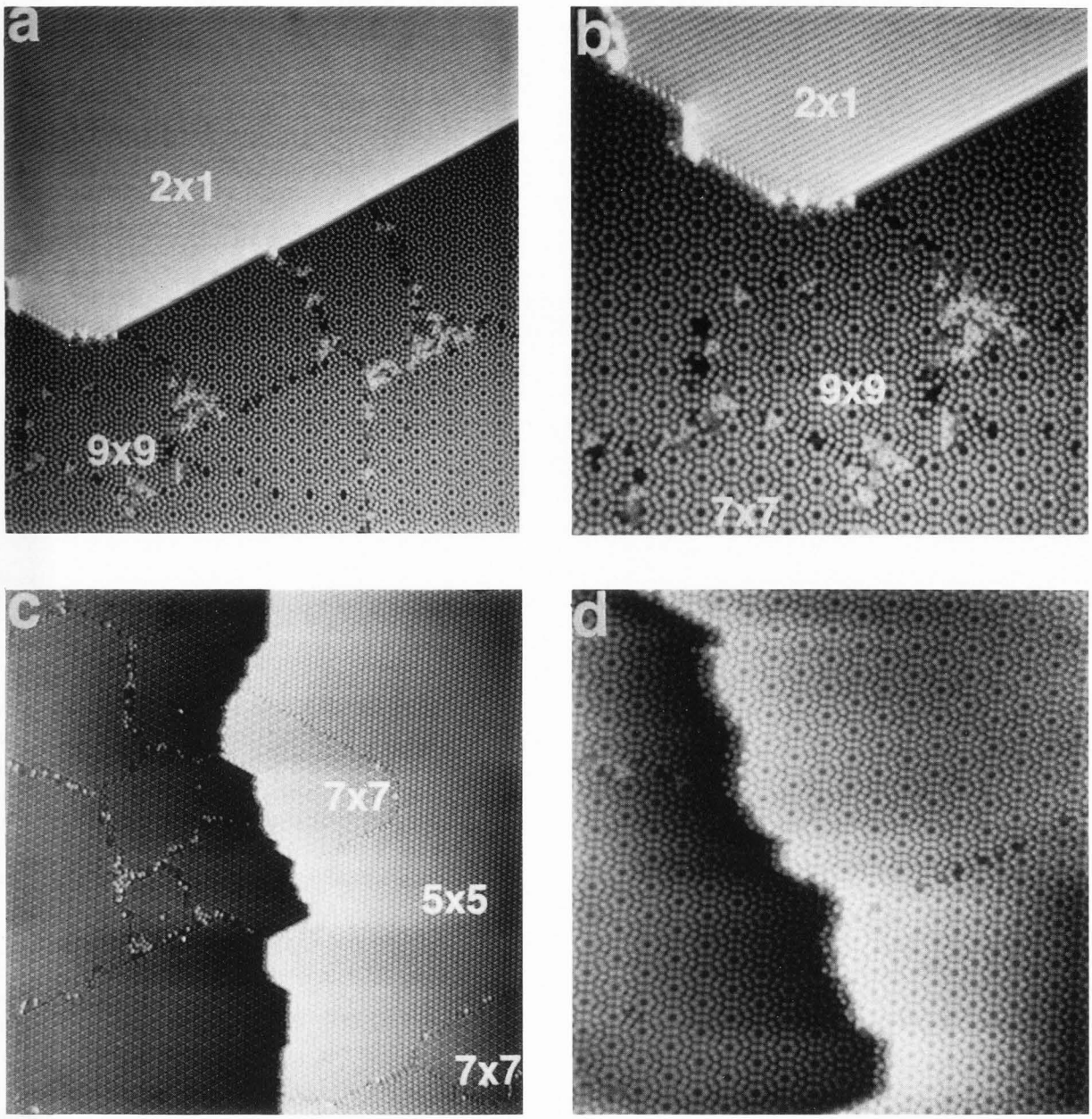

Figure 3. (a) and (b): Images of island A showing 2x1 reconstruction on the island surrounded by small 7x7 domains with one 9x9 domain in the surface layer. (c) and (d): These figures show that the structure of island B consists of 5x5 and 7x7. Image sizes: 50 nm x 50 nm (a); 30 nm x 30 nm (b and d); and 100 nm x 100 nm (c).

---

incorporated into an ordered layer. The width of the depletion zone seen in Figures 2a and 2b measures ~220 nm. Thus, the minimum width of a terrace needed to trap the Si adatoms at the specified cooling rate of 100°C/s, is ~440 nm. On a uniformly stepped surface, this would correspond to a miscut angle less than 0.04° which is impractical to obtain by mechanical cutting and polishing. An atomically resolved image of the 7x7 regions and a small "cloudy" region is shown in Figure 2c. The bright features in the "cloudy" region appear to contain a disordered overlayer of bright triangular features of atomic scale with 2x2/c2x4 type reconstructions in the underlying surface layer. The atomically resolved filled and empty-state images of these features are quantitatively different from the "ring" structures observed in the presence of Ni and Co (Wilson and Chiang, 1987; Bennett *et al.*, 1992). To confirm that these structures are not due to metal contamination, we have performed

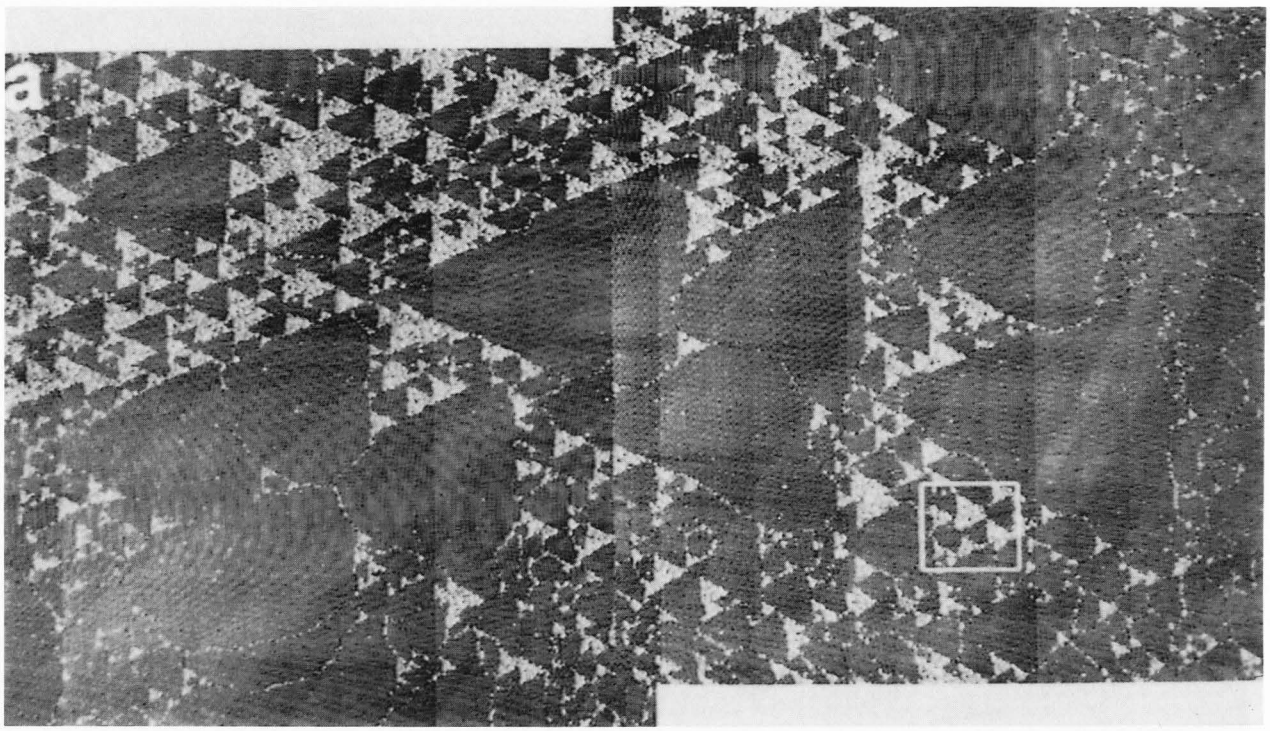

Figure 4 (a, above; b-e on the facing page). (a) 1400 nm x 750 nm scan of area far away from the islands shown in Figure 2d where there is still some remaining cloudiness. In addition to large 7x7 triangular domains, there are many small triangular regions in the high atom density regions. (b) Close-up of an area (150 nm x 150 nm) in the lower-left corner of the image shown in (a) where the local adatom density is low as indicated by the existence of very few cloudy regions in the area. A small domain of 9x9 found in the center of the image is surrounded by 7x7 domains. Sample biases are -2 V in (a) and (b). (c) and (d) Atomically resolved images of the same area [scan sizes: 50 nm x 50 nm (in c) and 30 nm x 30 nm (in d)]. (e) Six units of 11x11 are shown along with many domains of 9x9 and 7x7 (scan size: 50 nm x 50 nm). The insert shows a half unit of 13x13. Sample biases for (c)-(e) are +2 V.

---

careful annealing experiments on surfaces with and without Ni contamination (Yang and Williams, unpublished results). The STM signature of Ni contamination is very clear: on annealed contaminated surfaces, Ni-induced ring structures are clustered near steps and domain boundaries. No such structures were observed following annealing of the clean surfaces used in this work. From these observations, we estimate that the upper limit of the amount of Ni on these surfaces cannot be more than 0.01 monolayer (ML) at the 95% confidence level.

To confirm that the bright features observed following rapid cooling are indeed Si atoms trapped in the overlayer, surfaces such as the one shown in Figures 2a-2c were annealed at 600°C for 2 minutes. The resulting surface exhibits formation of islands as shown in Figure 2d. Simultaneously, the amount of "cloudy" region on these reannealed surfaces is also reduced as shown in the close-up image of Figure 2e. A depletion zone of cloudy areas is clearly present around each island in Figure 2e. These results provide direct evidence that the "1x1" phase has higher atom density than the 7x7 phase. Based on our measured 6% area coverage of the islands from STM images and assuming all islands have 7x7 reconstruction, the atom density difference between the "1x1" and the 7x7 is 0.06 (6%) (Yang and Williams, 1994). Taking into account that the 7x7 atom density is ~4% higher than that of the 1x1, we thus estimate that the density of the high temperature "1x1" phase is about 10-11% more than the bulk-terminated 1x1 atom density. This density difference of 0.10-0.11 double-layers would correspond to an adatom density of 0.2-0.22 ML. The uncertainty in the estimation is due to several factors. First, as we will show, there are different structures with different atom densities in the surface layer and islands. Second, there are still some remaining "cloudy" areas in the region far away from the islands and step edges, as evident in Figures 2d and 2e. The low and high limits of the measured density correspond to when these contributions are ignored and when they are over-estimated from our STM images, respectively.

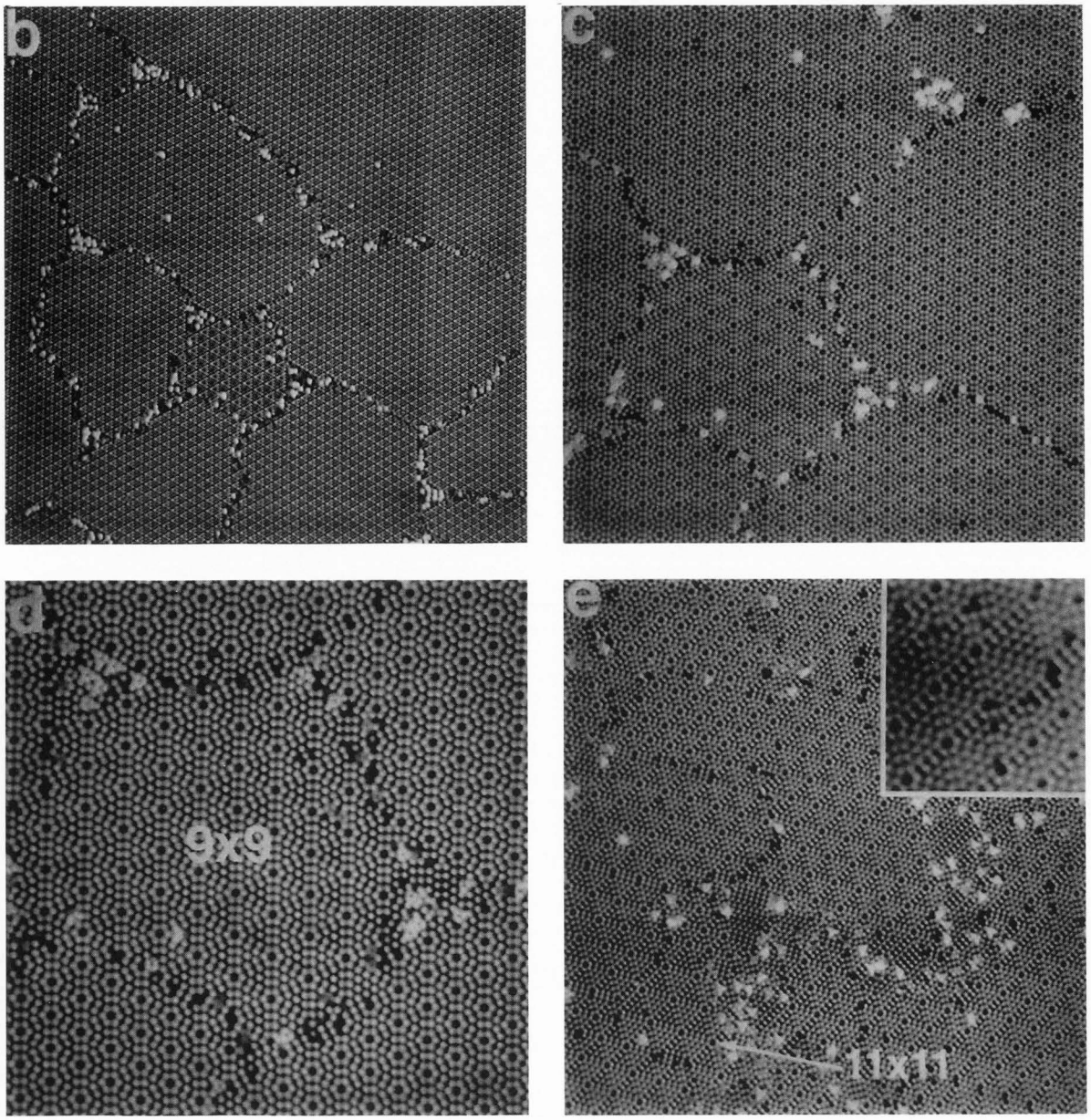

Reconstructions in the islands

The excess atom density found on large terraces after the quench also appears to cause the formation of non-equilibrium reconstructions. First, the islands shown in Figures 2d and 2e are composed of different reconstructions. This can be observed in the large area scans in Figures 2d and 2e where island A in the images clearly has lower island height than other islands on the same terrace. A close-up image of island A (Fig. 3a) shows that it has a 2x1 reconstruction with the 2x rows clearly resolved (Feenstra *et al.*, 1987; Yokoyama *et al.*, 1994). The island is mostly surrounded by 7x7 in the surface layer with a small domain of 9x9 found near the left-lower corner of the island. A smaller area scan shown in Figure 3b reveals each individual unit cell of 2x1 (Feenstra *et al.*, 1987). Although islands B and C appear to have the same height in large area scans (such as the ones shown in Figs. 2a and 2b), small area images reveal that island B represents a mixture of 5x5 and 7x7 while island C is entirely composed of 7x7. Figure 3c shows a 150 nm x 150 nm scan of island B where two small domains of 7x7 and a large region of 5x5 on the island are clearly evident. An atomically resolved image of 7x7 and 5x5 on the island is shown in Figure 3d. We note that both the 2x1 and the 5x5 have lower atom density than that of the 7x7, and have also been observed during epitaxial growth (Hoegen *et al.*, 1989;

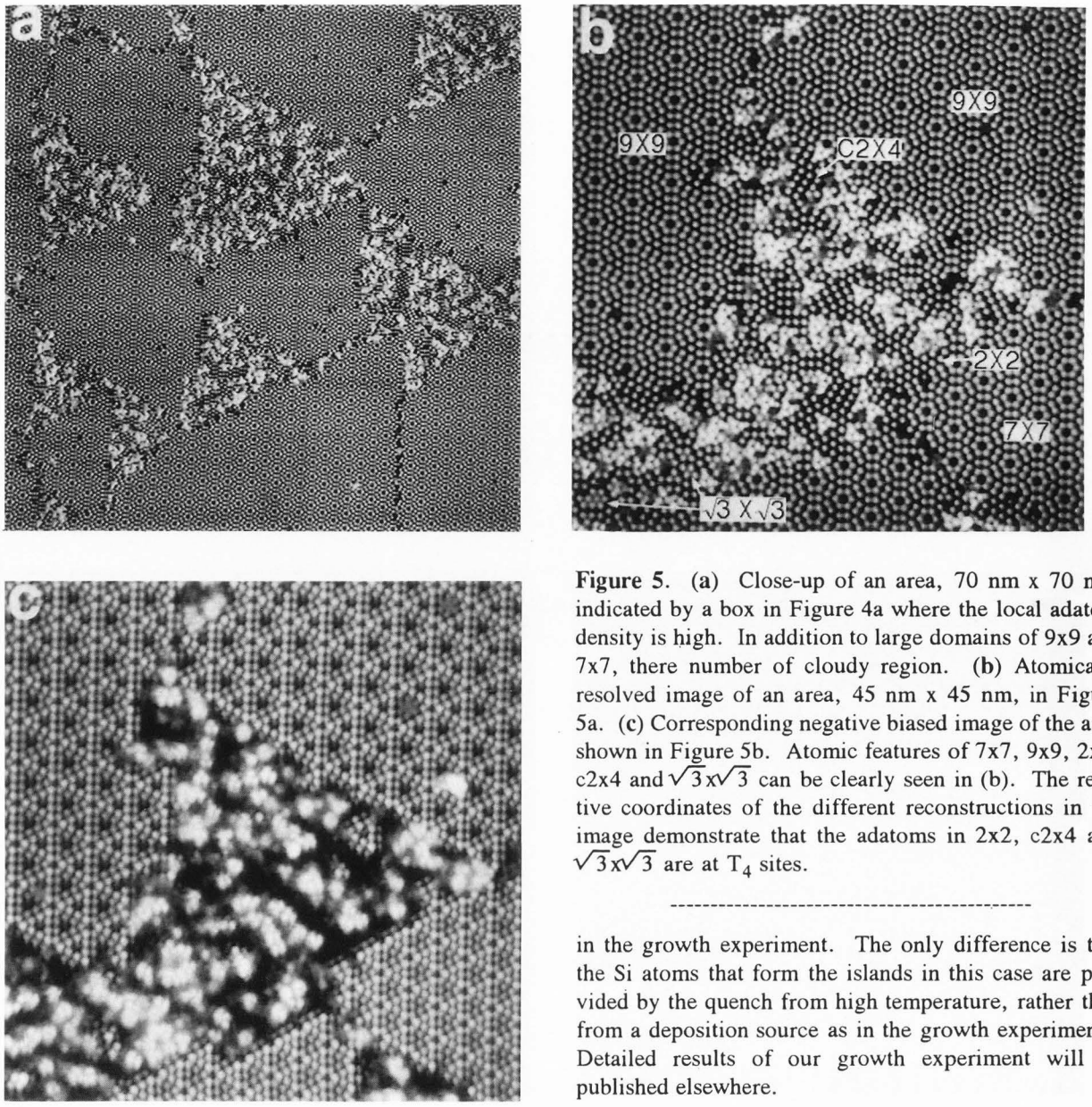

Figure 5. (a) Close-up of an area, 70 nm x 70 nm, indicated by a box in Figure 4a where the local adatom density is high. In addition to large domains of 9x9 and 7x7, there number of cloudy region. (b) Atomically resolved image of an area, 45 nm x 45 nm, in Figure 5a. (c) Corresponding negative biased image of the area shown in Figure 5b. Atomic features of 7x7, 9x9, 2x2, c2x4 and $\sqrt{3}x\sqrt{3}$ can be clearly seen in (b). The relative coordinates of the different reconstructions in the image demonstrate that the adatoms in 2x2, c2x4 and $\sqrt{3}x\sqrt{3}$ are at T_4 sites.

Yang and Williams, 1994; Yokoyama *et al.*, 1994). The surface densities of various reconstructions are shown in Table 1. In the present quench and anneal experiment, they have only been found on the islands and never in the surface layer. It will become clear later why the low atom density of 2x1 and 5x5 precludes the possibility of having them in the surface layer. From other studies of growth, we have found that the formation of 2x1 and 5x5 islands is related to the domain boundaries in the substrate. As is evident from Figures 2 and 3, there is no shortage of domain boundaries on the quenched surface, especially in the "cloudy" regions. Thus, we conclude the cause of the formation of 2x1 and 5x5 islands in the present experiment is the same as that in the growth experiment. The only difference is that the Si atoms that form the islands in this case are provided by the quench from high temperature, rather than from a deposition source as in the growth experiments. Detailed results of our growth experiment will be published elsewhere.

Reconstructions in the surface layer

As Figures 3a-3d show, the reconstruction in the surface layer near islands is mostly 7x7 with occasional 9x9 regions. However, in the regions that are far away from the islands, non-7x7 reconstructions are frequently found. Figure 4a shows a scan taken from one such area in Figure 2e where there are still some "cloudy" structures. Each large dark triangular-shaped area ($\sim$300 nm in size) represents a single domain of 7x7 formed when the surface was quenched from high temperature. In the "cloudy" regions, there are alternating dark and bright small triangles ($\sim$30 nm in size). These features must have developed when the sample was reannealed at 600°C, because on the surfaces without reannealing such small triangles are absent.

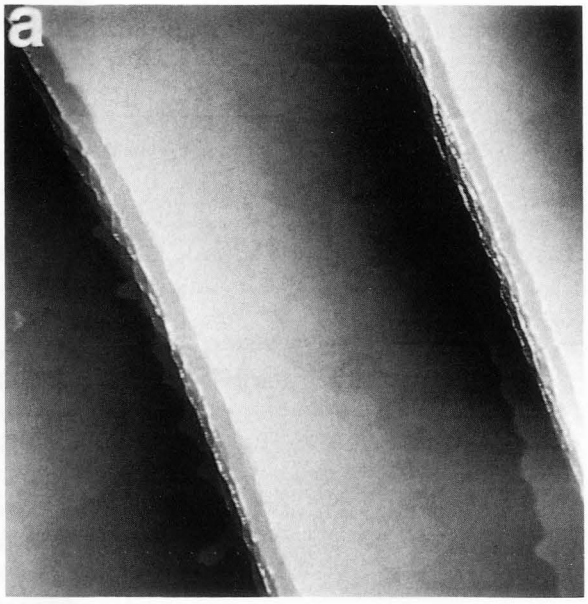

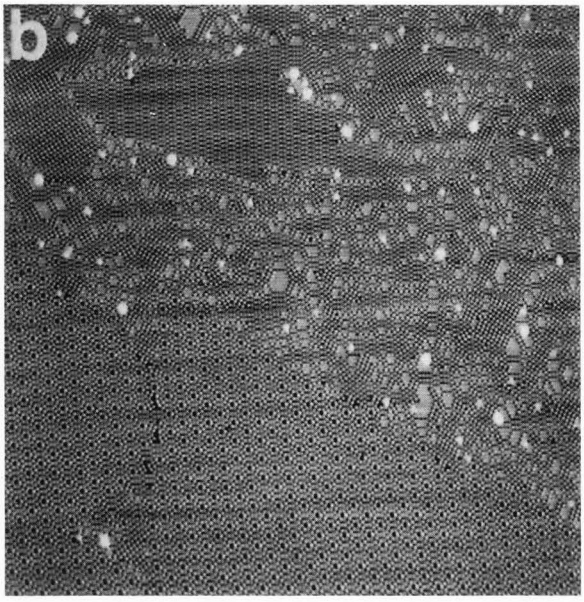

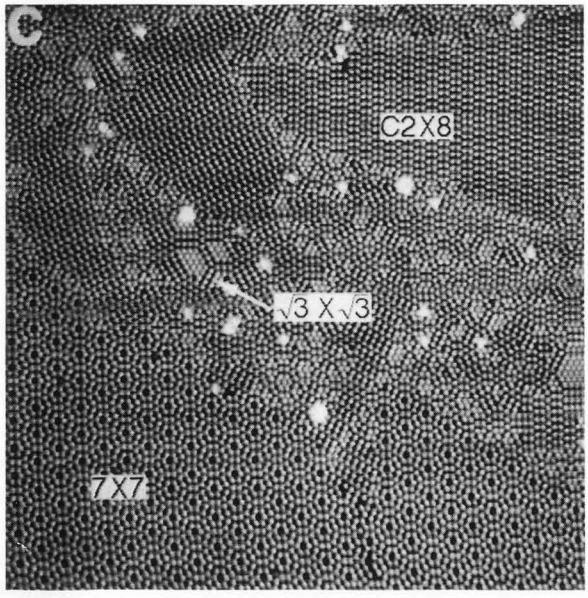

Figure 6. (**a**) 2000 nm x 2000 nm image of surface quenched with a slower rate than was used for the surface shown in Figure 2a. The terrace size here is also smaller, ~ 1000 nm compared to 2000 nm in Figure 2a. Due to the negative bias of -2 V, the bright gray scale corresponds to the 7x7 region and dark triangles are the regions with high density reconstructions. Sample bias is -2 V. (**b**) Atomically resolved 100 nm x 100 nm image of the 7x7 and the region with high atom density showing c2x8, 2x2, c2x4 and $\sqrt{3}x\sqrt{3}$. It is interesting to note that the large domains in the high density region all have c2x8 reconstruction, indicating that c2x8 has lower energy than 2x2 and c2x4, as the atom densities for all three are the same. (**c**) A close up view of the c2x8 and $\sqrt{3}x\sqrt{3}$ (scan size: 60 nm x 60 nm). The sample biases for (b) and (c) are +2 V.

Figures 4b-4d show a sequence of close-up STM images of an area in the lower-left corner of Figure 4a where the cloudiness is relatively small. In the occupied state image of Figure 4b, the 7x7 domains appear as ordered areas with small diamond-shaped units. The unit cell consists of a dark and a bright triangle under the imaging condition of -2 V sample bias, caused by the stacking fault in half of the cell. The 9x9 domain in the center of the image has almost the same appearance as the 7x7 except with a larger unit cell, indicating the existence of a stacking fault in the 9x9. The unoccupied state images of Figures 4c and 4d further confirm that the 9x9 reconstruction is of Takayanagi type, as expected: namely, it consists of adatoms and corner holes and half of the unit cell has a stacking fault. The 9x9 can be best distinguished from the 7x7 in Figure 4d by noting that there are 4 pairs of adatoms between any two corner holes while there are only 3 for the 7x7. Figure 4e shows 6 units of the previously unreported 11x11 reconstruction that was found from a region similar to that of Figures 4b-4d. The 11x11 has an appearance similar to the 9x9 and 7x7 and it can be easily identified in the image by the fact that there are 5 pairs of adatoms between any two corner holes. The insert in Figure 4e shows half a unit cell of 13x13 structure that was found on a different part of the same surface.

Figure 5a shows a close-up image of a cloudy region on the surface indicated by the square box in Figure 4a. The sample bias voltage has been changed from

-2 V in Figure 4a to +2 V, namely, the image is probing the unoccupied state. In addition to the 7x7, several 9x9 domains, as large as 71 unit cells, are present on the surface. The third type of region present (cloudy triangles) appears to consist of randomly distributed adatoms on a surface that has non-Takayanagi type structures. An image at larger magnification (Fig. 5b) shows that the structure of these regions consists of 2x2 and c2x4 in the surface layer with some adatoms on top of the surface. A more careful inspection of Figure 5b reveals that there are also small regions of $\sqrt{3}$x$\sqrt{3}$ as seen in the lower left part of the image. The way to distinguish the $\sqrt{3}$x$\sqrt{3}$ from the 2x2 is by noting that the dimension of the cell is smaller for $\sqrt{3}$x$\sqrt{3}$ and that the orientation of the $\sqrt{3}$x$\sqrt{3}$ unit cell is rotated 30° from that of the 2x2. An occupied state image of the same area is shown in Figure 5c. Apparently, the image of occupied state is more sensitive to the overlayer of trapped Si atoms, while unoccupied state image makes the structures in the surface layer more pronounced. In the occupied state image of Figure 5c, the two halves of the 7x7 unit cell have different apparent heights. The brighter half represents the unfaulted half. By comparing images in Figures 5b and 5c, the corresponding unfaulted half of 7x7 in Figure 5b can be identified. Since the unoccupied image reflects the position of adatoms and adatoms in the 7x7 are at T4 sites, from the relative position of the adatoms in 2x2, c2x4 and $\sqrt{3}$x$\sqrt{3}$ to that of the 7x7, we conclude that they also occupy the T4 sites, as expected from theoretical calculation (Meade and Vanderbilt, 1989a,b).

In addition to the observation of various reconstructions, the electronic structure exhibited by the 9x9 in the STM can be observed in agreement with previous reports (Becker *et al.*, 1989). The 9x9 reconstruction differs from the 7x7 structure in that there is an adatom in the center of the 9x9 half cell that is surrounded by other adatoms, which we will call the center adatom. From the Takayanagi model, this means that the center adatom is not adjacent to any subsurface defects, such as dimer rows and corner holes. Inspection of Figures 5b and 5c reveals that although such an adatom has the same appearance as other adatoms in the unoccupied state image of Figure 5b, it appears as a depression in the occupied state image (Fig. 5c). In the upper right corner of Figure 5b, two of such center adatoms are missing, and the entire corresponding half cells appear depressed in Figure 5c. We also notice that the 2x2/c2x4 in Figure 5c appear to be depressed and that adatoms in the 9x9 are locally in a 2x2 configuration. All of these observations seems to suggest that the charge is transferred to non-center adatoms in the 7x7 and 9x9 from their neighboring defects.

An Energetic Model For the Formation of Non-7x7 Reconstructions in the Surface Layer

Table 1 lists the atom densities for all the reconstructions that have been observed on Si(111). As noted above, a striking correlation is that the observed metastable (non-7x7) reconstructions in the surface layer, namely 9x9, 11x11, 2x2, c2x4 and $\sqrt{3}$x$\sqrt{3}$, all have higher densities than the 7x7 (reconstructions that have lower atom densities than 7x7, such as 5x5 and 2x1, were never found in the surface layer, only as islands on top of the surface layer). Furthermore, regions with high local density of trapped Si atoms in the overlayer (Fig. 5a) contain higher percentages of high-atom-density reconstructions compared to regions with lower adatom density where few high density structures are found (Fig. 4b). Given these observations, it is reasonable to deduce that the metastable structures in the surface layer form to accommodate a high density of adatoms trapped during the quench. This is similar in philosophy to the previous Feenstra and Lutz's conclusion that the low density 5x5 structure forms from the cleaved 2x1 due to a low density of atoms present on the surface (Feenstra and Lutz, 1990, 1991b), and similar to a recent report of changes in the reconstruction of Pt(111) due to deposited Pt atoms (Bott *et al.*, 1993).

The process in which the metastable reconstructions are formed in this experiment can then be understood as follows: during the phase transition, the 7x7 and "1x1" structures are known to coexist (Bauer *et al.*, 1991). Thus, when the 7x7 is first formed on the terrace, it absorbs some of the excess atoms and pushes the remainder aside to regions that are still in the "1x1" phase, creating an abnormally high atom density in those regions. During the quench, such regions order locally into a surface layer with high density reconstructions and a trapped Si overlayer which appears bright in the STM images. When the surface is reannealed at moderate temperature, there is sufficient atomic mobility to allow the system to lower its energy by creating more ordered structures, subject to the constraint of the high atom density in the region imposed by the limited diffusion length. The formation of higher density structures such as 9x9 accommodates some of the excess atoms (see Table 1) and the remaining excess adatoms are further pushed into the remaining cloudy region, creating an even higher atom density in this region. As a result, reconstructions with even higher atom densities such as 2x2, c2x4 and $\sqrt{3}$x$\sqrt{3}$ are formed in these regions. Experimentally, additional adatoms were only observed on top of the regions that have 2x2, c2x4 and $\sqrt{3}$x$\sqrt{3}$ reconstructions following annealing. This mechanism is also consistent with previous observation of some of these reconstructions during growth where the high atom

density was achieved through supersaturation (Kahata and Yagi, 1989; Kohler *et al.*, 1989; Feenstra and Lutz, 1991a).

To understand how the formation of metastable structures can be driven by an excess atomic density, for simplicity, we model the formation of the 9x9 by considering an area A on the surface having an atom density so that it can be completely filled with 9x9. An alternative configuration for the surface with the same number of atoms is to fill the area with 7x7, leaving a triangular 7x7 island on top, as the 7x7 atom density is smaller than that of the 9x9. Obviously, the only disadvantage for the later configuration, in terms of energetics, is that the steps at island edges cost energy. As a result, the energy cost of forming 7x7 with an island might be higher than that of the 9x9, which does not need to form island for the given atom density. Mathematically, for the 9x9 to be more favorable, we need to have

$$AE_9 < AE_7 + LE_s \qquad (1)$$

where E_9 and E_7 are the surface energy per 1x1 unit cell for the 9x9 and 7x7. E_s is the step energy per unit cell length for 7x7 island edges and L is the length of the island edge. It is assumed that the region under the island is 1x1, which is the zero of the energy scale. Assuming the island shape is an equilateral triangle and the total number of atoms is conserved in different configurations, the length of the island edge can be related to the area through

$$L = \alpha\sqrt{A} \qquad (2)$$

where

$$\alpha = [(36\ D_9 - D_7) / (\sqrt{3} D_1)]^{1/2} = 0.659 \qquad (3)$$

where D_9, D_7, and D_1 refer to the atom density per 1x1 unit cell for 9x9, 7x7 and 1x1 listed in the second column of Table 1. It is clear from eq. (3), α increases as the surface atom density, which in this case is D_9, increases. Thus, combining eqs. (1)-(3), the requirement for stabilizing the 9x9 structure is

$$E_9 - E_7 < [(\alpha E_s)/(\sqrt{A})] \qquad (4)$$

From Eq.(4), it is clear that formation of the higher energy 9x9 structure can be stabilized with respect to formation of a 7x7 region with a 7x7 island. The area of the region that can be stabilized will be governed by the edge energy of the island. The equation also allows us to estimate the energy difference between the 7x7 and 9x9. If we use the estimate of $E_s = 0.211$ eV/unit cell length (Williams *et al.*, 1993) and let A = 81 N, where N is the number of 9x9 unit cells in area A, we get

$$E_9 - E_7 < (0.015 / \sqrt{N})\ \text{eV} \qquad (5)$$

Experimentally, as many as 71 units of 9x9 have been found in a single domain. Using this number, we estimate from eq. (5), that $E_9 - E_7 < 0.002$ eV per 1x1 cell. Previous calculations of the energies of the reconstructions of Si(111) (Vanderbilt, 1987) allow the energy difference between $E_9 - E_7$ to be determined as 0.005 eV. In addition, the calculated energy difference between 9x9 and 7x7 for Ge(111) is -0.004 eV (Mercer and Chou, 1993; note the different sign). Both of the calculated values are of the same order of magnitude as the value we estimated for Si(111). In addition, our estimated energy difference between 9x9 and 7x7 for Si(111) is of the same order of magnitude as the calculated energy differences between other Takayanagi structures ($\sim$10 meV/1x1 cell) (Brommer *et al.*, 1992; Stich *et al.*, 1992). The estimated value using eq. 4 is directly proportional to the value of E_s which is not precisely known. The E_s value we have used could easily be a factor of 2 too small due to the method used to deduce it. The same idea can easily be used to argue for the formation of other reconstructions we have observed in the surface layer. Since the observed sizes for 11x11, 2x2, c2x4 and $\sqrt{3}$x$\sqrt{3}$ are all much smaller than that of the 9x9, use of eq. 4 leads to the conclusion that the surface energies for these reconstructions should be higher than that of the 9x9 as would be expected.

Creating Large Areas of 2x2/c2x4/c2x8 and $\sqrt{3}$x$\sqrt{3}$

The essence of the argument presented in the last section shows that a metastable reconstruction can be stabilized over lower energy reconstructions if the atom density in the area matches that of the particular reconstruction. From Table 1, we note that our measured atom density for the high temperature "1x1" is slightly smaller than that of the 2x2/c2x4. Thus, in principle, we should be able to stabilize the 2x2/c2x4 by obtaining areas on the surface having the atom density of the 2x2/c2x4, even though the energy of 2x2/c2x4 is certainly higher than 7x7 and 9x9. However, the fast quench rate (100°C/s) we have used results in homogeneous nucleation of 7x7 on the terraces (Yang and Williams, 1994). As a result, the atom density on the non-7x7 region is higher than that of the 2x2/c2x4 and lower energy reconstructions plus island become more favorable. Therefore, the key to create large regions of 2x2 type reconstructions may be to keep the atom density in the remaining "1x1" region below that of the 2x2 by preventing too many 7x7 regions nucleating in the middle region of the terrace. Since for slow cooling rate (0.5°C/s), the 7x7 only nucleates from the step top (Bauer *et al.*, 1991), we can expect a cooling rate between the slow rate (0.5°C/s) and fast rate (100°C/s) may achieve the goal of creating the non-7x7 regions

having an atom density equal to that of the 2x2/c2x4 after quench.

Experimentally, we decrease the quench rate to ~70°C/s by increasing the sample mass and at the same time decreasing the size of the terrace between two step bunches to ~1000 nm. Si(111) quenched using this configuration is shown in Figure 6a. There are two apparent gray scales, namely, the dark triangles and higher gray-scale region that includes areas near step edges. Atomically resolved images show that the regions with bright gray scale correspond to the 7x7 while the dark triangles contain high density reconstructions, such as 2x2. The different appearance of the various regions is a result of negative sample bias voltage used. In comparison to Figure 2a, the surface shown in Figure 6a has larger 7x7 domains with most of them close to the step edges. An area, which includes the boundary between the 7x7 and a high density region, is shown in Figure 6b and a closer-up image is shown in Figure 6c (+2 V sample bias). Indeed, large regions of 2x2 type reconstruction are found on the surface. However, careful inspection of Figure 6c reveals that the reconstruction of large areas is c2x8 instead of 2x2 or c2x4. The c2x8 has exactly the same atom density as the 2x2 and c2x4 (it can be thought to consist of alternating 2x2 and c2x4 cells). Previously, only 2x2 and c2x4 have been reported (Becker *et al.*, 1986; Kohler *et al.*, 1989). There are also many regions of $\sqrt{3}x\sqrt{3}$ that are much larger than we have seen before, which represents the attempt by the surface to keep all the atoms in the surface by having higher atom density reconstruction. It is also clear from Figure 6 that there are almost no atoms being ejected from the surface which is what is needed to stabilize the 2x2 type structures according to our earlier analysis.

Conclusion

In conclusion, by creating unusually large terraces using electromigration, we have shown that the atom density in the high temperature "1x1" phase for Si(111) is about 6% higher than the 7x7. This is about 10-11% higher than the bulk-terminated 1x1. By removing the steps which otherwise act as sinks for excess atom density, we have demonstrated that we can utilize the existence of this high atom density at high temperature to create areas of 9x9, 2x8 and $\sqrt{3}x\sqrt{3}$ larger than have been seen before. We have also created structures that have never been reported before on Si(111), such the 11x11, 13x13 and c2x8. We have found that the c2x8 is similar in energy to other members of the 2x2/c2x4/2x8 structure family. Through examination of the relative locations of these reconstructions, we were able to conclude from the experimental data that these non-7x7 reconstructions are stabilized by the artificially-created abnormally high atom density on the surface. Simple energetic arguments which consider the atom density are shown to be consistent with such a conclusion.

Acknowledgements

The authors thank Norman C. Bartelt for many useful discussions and Elain Fu for helping in preparing figures. This work was supported by the Office of Naval Research.

References

Alfonso C, Bermond JM, Heyraud JC, Métois JJ (1992). The meandering of steps and the terrace width distribution on clean Si(111). An *in situ* experiment using reflection electron microscopy. Surf. Sci. **262**: 371-381.

Bauer E, Mundschau M, Swiech W, Telieps W (1991). Low-energy electron microscopy of semiconductor surfaces. J. Vacuum Sci. Technol. **A9**: 1007-1013.

Becker RS, Golovchenko JA, Hamann DR, Swartzentruber BS (1985). Real space observation of surface states on Si(111)-7x7 with the tunneling microscope. Phys. Rev. Lett. **55**: 2032-2034.

Becker RS, Golovchenko JA, Higashi GS, Swartzentruber BS (1986). New reconstructions on silicon (111) surfaces. Phys. Rev. Lett. **57**: 1020-1023.

Becker RS, Swartzentruber BS, Vickers JS, Klitsner T (1989). Dimer-adatom-stacking-fault (DAS) and non-DAS (111) semiconductor surfaces: A comparison of Ge(111)-c(2x8) to Si(111)-(2x2), -(5x5), -(7x7), and -(9x9) with scanning tunneling microscopy. Phys. Rev. **B39**: 1633-1647.

Bennett PA, Webb MB (1981). The Si(111) 7x7 to 1x1 transition. Surf. Sci. **104**: 74-104.

Bennett PA, Copel M, Cahill D, Falta J, Tromp RM (1992). Ring clusters in transition metal silicon surface structures. Phys. Rev. Lett. **69**: 1224-1227.

Bott M, Hohage M, Michely T, Comsa G (1993). Pt(111) reconstruction induced by enhanced Pt gas-phase chemical potential. Phys. Rev. Lett. **70**: 1489-1492.

Brommer KD, Needels M, Larson BE, Joannopoulos JD (1992). *Ab initio* theory of the Si(111)-7x7 surface reconstruction: A challenge for massively parallel computation. Phys. Rev. Lett. **68**: 1355-1358.

Feenstra RM, Lutz MA (1990). Formation of the 5x5 reconstruction on cleaved Si (111) surfaces studied by scanning tunneling microscopy. Phys. Rev. **B42**: 5391-5394.

Feenstra RM, Lutz MA (1991a). Deposition and annealing of silicon on cleaved silicon surfaces studies by scanning tunneling microscopy. In: The Structure of

Surfaces III. Tong SY, Van Hove MA, Xie SC (eds.). Springer-Verlag, Berlin. pp. 480-485.

Feenstra RM, Lutz MA (1991b). Kinetics of the Si(111)2x1 → 5x5 and 7x7 transformation studied by scanning tunneling microscopy. Surf. Sci. **243**: 151-165.

Feenstra RM, Stroscio JA, Fein AP (1987). Tunneling spectroscopy of the Si(111)2x1 surface. Surf. Sci. **181**: 295-306.

Hamers RJ, Tromp RM, Demuth JE. (1986). Surface electronic structure of Si(111)-(7x7) resolved in real space. Phys. Rev. Lett. **56**: 1972-1975.

Hoegen MHV, Falta J, Henzler M (1989). The initial stages of growth of silicon on Si(111) by slow positron annihilation low-energy electron diffraction. Thin Sol. Films **183**: 213-220.

Homma Y, McClelland RJ, Hibino H (1990). DC-resistive heating induced step bunching on vicinal Si (111). Jpn. J. Appl. Phys. **29**: L2254-L2256.

Ino S (1977). Some new techniques in reflection high energy electron diffraction (RHEED): Application to surface structure studies. Jpn. J. Appl. Phys. **16**: 891-908.

Iwasaki H, Hasegawa S, Akizuki M (1987). Diffuse scattering in the high-temperature (1x1) state of Si (111). J. Phys. Soc. Jpn. **56**: 3425-3428.

Kahata H, Yagi K (1989). The Effect of surface anisotropy of Si(001) 2x1 on hollow formation in the initial stage of oxidation as studied by reflection electron microscopy. Surf. Sci. **220**: 131-136.

Kohler U, Demuth JE, Hamers RJ (1989). Scanning tunneling microscopy study of low-temperature epitaxial growth of silicon on Si(111)-7x7. J. Vacuum Sci. Technol. **A7**: 2860-2867.

Lander JJ (1964). Chemisorption and ordered surface structures. Surf. Sci. **1**: 125-129.

Latyshev AV, Aseev AL, Krasilnikov AB, Stenin SI (1989). Transformations on clean Si(111) stepped surface during sublimation. Surf. Sci. **213**: 157-169.

Latyshev AV, Krasilnikov AB, Aseev AL, Sokolov LV, Stenin SI (1991). Reflection electron microscopy study of clean Si(111) surface reconstruction during the 7x7 to 1x1 phase transition. Surf. Sci. **254**: 90-96.

Meade RD, Vanderbilt D (1989a). Adatoms on Si(111) and Ge(111) surfaces. Phys. Rev. **B40**: 3905-3913.

Meade RD, Vanderbilt D (1989b). Origins of stress on elemental and chemisorbed semiconductor surfaces. Phys. Rev. Lett. **63**: 1404-1407.

Mercer JL, Chou MY (1993). Energetics of the Si(111) and Ge(111) surfaces and the effect of strain. Phys. Rev. **B48**: 5374-5385.

Noh DY, Blum KI, Ramstad MJ, Birgeneau RJ (1993). Faceting, roughness, and step disordering of vicinal Si(111) surfaces: An X-ray scattering study. Phys. Rev. **B48**: 1612-1625.

Pandey KC (1981). New π-bonded chain model for the Si(111)-(2x1) surface. Phys. Rev. Lett. **47**: 1913-1917.

Phaneuf RJ, Williams ED (1987). Comparison of high-temperature and laser-quenched Si(111) using low-energy electron diffraction. Phys. Rev. **B35**: 4155-4158.

Schlier RF, Farnsworth HE (1959). Structure and adsorption characteristics of clean surfaces of germanium and silicon. J. Chem. Phys. **30**: 917-926.

Stich I, Payne MC, King-Smith RD, Lin J-S, Clarke LJ (1992). *Ab initio* total-energy calculations for extremely large systems: Application to the Takayanagi reconstruction of Si(111). Phys. Rev. Lett. **68**: 1351-1354.

Takayanagi K, Tanishiro Y, Takahashi M, Takahashi S (1985). Structural analysis of Si(111)-7x7 by UHV-transmission electron diffraction and microscopy. J. Vacuum Sci. Technol. **A3**: 1502-1506.

Vanderbilt D (1987). Model for the energetics of Si and Ge(111). Phys. Rev. **B36**: 6209-6212.

Williams ED, Phaneuf RJ, Wei J, Bartelt NC, Einstein TL (1993). Thermodynamics and statistical mechanics of the faceting of stepped Si(111). Surf. Sci. **294**: 219-242.

Wilson RJ, Chiang S (1987). Surface modifications induced by adsorbates at low coverage: A scanning tunneling-microscopy study of the Ni/Si(111)-Sqrt(19) surface. Phys. Rev. Lett. **58**: 2575-2578.

Yang YN, Williams ED (1994). High atom density in the 1x1 phase and origin of the metastable reconstructions on Si(111). Phys. Rev. Lett. **72**: 1862-1865.

Yokoyama T, Tanaka H, Itoh M, Yokotsuka T, Sumita I (1994). Scanning-tunneling-microscope observation of 2x1 structure on a homoepitaxially grown Si(111) surface. Phys. Rev. **B49**: 5703-5705.

Discussion with Reviewers

D. Vanderbilt: A puzzling aspect of this work is the observation of reconstructions on top of the islands (e.g., 2x1 and 5x5) which have **low** atom density, thus suggesting that the island tops are in a subsaturated condition at the same time the terraces are in a supersaturated condition. Do the authors have any suggestions why this may be occurring? For example, is it possible that strong asymmetries in the attachment kinetics at a step from below and above may play a role?
Authors: The low density reconstructions are observed in islands that have nucleated at domain boundaries of the reconstruction of the substrate. It may be that the domain boundaries are regions of low density, thus creating the low-density conditions needed to stabilize these reconstructions. It may also be the case that the

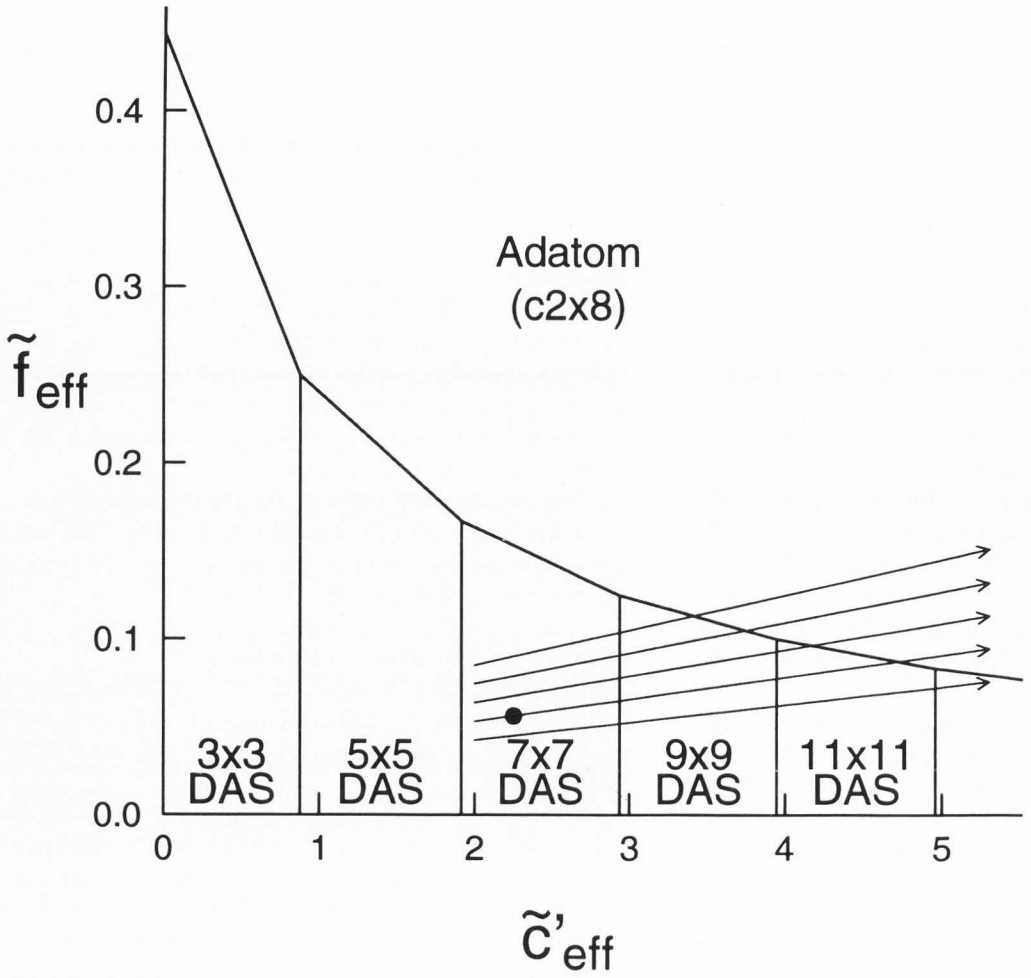

Figure 7. Model phase diagram of surface structures for the Si(111) surface; c'_{eff} and $\bar{f}$ are measures of the corner hole and stacking fault energies respectively. Arrows show trajectories which are traversed as the chemical potential μ for excess silicon atoms in the surface layer is varied.

reduced symmetry of the substrate due to the domain walls helps stabilize the lower-symmetry 2x1 structure.

D. Vanderbilt: Perhaps a useful way to think about the effects observed here is to introduce a "chemical potential" μ for Si atoms in the surface layer. Usually μ is pinned to the bulk cohesive energy by step-mediated exchange with the bulk "reservoir", but by preparing very wide terraces, a supersaturated condition ($\mu > \mu_{bulk}$) is apparently reached. From this point of view, it seems likely that some of the structures observed, such as the 9x9, are the quasi-equilibrium structures which occur when μ is increased while out of contact with the bulk reservoir. For example, the simple empirical theory of Vanderbilt (1987) gives the energy per 1x1 cell as

$$\Delta E_{DAS} = \Delta f/2 + (2n\Delta w + \Delta c') / (2n+1)^2,$$

where Δf, Δw, and $\Delta c'$ are measures of the faulting energy, domain wall formation energy, and corner hole formation energy, respectively. The excess density of atoms in the surface layer per 1x1 cell, relative to the simple adatom phases, is

$$\Delta N_{DAS} = -(8n+ 9)/4(2n+1)^2.$$

Minimizing the free energy $\Delta E_{DAS} - \mu\Delta N_{DAS}$ is thus exactly equivalent to minimizing the energy ΔE_{DAS} except that Δw and $\Delta c'$ must be replaced by $\Delta w_{eff} = \Delta w + \mu$ and $\Delta c'_{eff} = \Delta c' + 9\mu/4$, respectively. The loci of values of Δw_{eff} and c'_{eff} as μ increases form straight lines, is shown in Figure 7. For a reasonable value of parameters (filled circle), the quasi-equilibrium structure evolves from 7x7 to 9x9 and 11x11 before converting to a simple adatom phase (c2x8). A slightly different choice of initial parameters could eliminate the 11x11 phase, or admit the 13x13. Conversely, a **reduction** of μ could drive a transition backwards into the 5x5 phase (or into the 2x1, not shown). Do the authors agree that this is a reasonable point of view?

Authors: This is a very useful construction for quantifying the effects of variable atomic density on the stability. As noted above, this construction may explain observations of the low-density 5x5 and 2x1 structures which form on islands which nucleate at domain boundaries.